# Sedimentation and Effective Temperature of Active Colloidal Suspensions

Jérémie Palacci, Cécile Cottin-Bizonne, Christophe Ybert, and Lydéric Bocquet
*LPMCN, Université de Lyon, Université Lyon 1 and CNRS, UMR 5586, F-69622 Villeurbanne, France*
(Received 18 April 2010; published 17 August 2010)

In this Letter, we investigate experimentally the nonequilibrium steady state of an active colloidal suspension under gravity field. The active particles are made of chemically powered colloids, showing self propulsion in the presence of an added fuel, here hydrogen peroxide. The active suspension is studied in a dedicated microfluidic device, made of permeable gel microstructures. Both the microdynamics of individual colloids and the global stationary state of the suspension under gravity are measured with optical microscopy. This yields a direct measurement of the effective temperature of the active system as a function of the particle activity, on the basis of the fluctuation-dissipation relationship. Our work is a first step in the experimental exploration of the out-of-equilibrium properties of active colloidal systems.

DOI: 10.1103/PhysRevLett.105.088304 PACS numbers: 82.70.Dd, 47.57.ef, 47.63.Gd

The collective behavior of ''active fluids'', made of self-propelled entities, has raised considerable interest over the recent years in the context of nonequilibrium statistical physics [1–10]. Such systems are rather common in living systems, from swimming cells and bacteria colonies [11,12], to flocks of birds or fishes [2]. These entities move actively by consuming energy and their behavior is thus intrinsically out of equilibrium. Building a general framework describing their collective properties remains accordingly a challenging task and has led to a considerable amount of work towards this aim [1–8]. By contrast, much less work has been performed on the experimental side, and mainly on assemblies of living microorganisms—which are naturally self-propelled [11–13], however at the expense of a lack of control and flexibility of the individual particles and their interactions. On the other side, experiments with collections of artificial motile systems mostly involved athermal self-propelled particles using vibrated asymetric grains [9,10]. There is therefore a need for new experiments at the colloidal scale, based on *artificial* model systems involving suspensions of microscopic active particles with controlled propulsion and interaction mechanisms—here designated as ''*active suspensions*.'' Several routes to design individual artificial microscopic swimmers have been explored recently [14–16], taking benefit of the recent progress made to design colloidal particles at microscales. However, going from the individual to the many particles situation remains a challenging task and has not been achieved up to now with artificial motile particles at the colloidal scale.

In this Letter we explore experimentally the behavior of a dilute active suspension of artificial swimmers under an external (gravity) field, allowing to address the applicability of thermodynamic concepts to active systems. In particular, we show that the properties of this system can be described within the framework of the fluctuation-dissipation relationships, with an effective temperature which is a probe of the injected power, in line with recent predictions [17]. The sedimentation of active particles was discussed theoretically in a recent contribution by Tailleur and Cates [8]. Here the active colloids are powered chemically, following the route proposed by Howse *et al.* [14]. The asymmetric dismutation of hydrogen peroxide ($H_2O_2$) on the colloid itself is used as the driving power, on the basis of a self (diffusio-) phoretic motion, induced by the building up of an osmotic pressure gradient at the interface of the colloid [18,19]. Furthermore, a specifically designed microfluidic system based on a gel-microdevice technology has been developed, allowing to ensure constant renewal of the chemical *fuel* ($H_2O_2$), as well as removal of *waste* products ($O_2$), in an open, convection-free, reactor configuration. On the basis of this device, we have explored the behavior of the active suspensions at two complementary levels: we have first characterized the individual dynamics of active colloids by particle tracking measurements; then we have investigated the behavior of a dilute active suspension of these particles under an external gravity force field, in the same spirit as the historical Jean-Perrin experiment [20]. This allowed us to connect the microdynamics of individual entities to the macroscopic equilibrium behavior of the suspension.

*Active colloids and experimental setup.*—A monolayer of commercial fluorescent latex colloids (1 $\mu$m diameter, Molecular Probes F8823) is formed on a silicon wafer by evaporation from $1{:}10^3$ dilution in isopropanol (99.99%, Roth), and coated with 2 nm platinum by sputtering; see Fig. 1(a). Resuspension is achieved by sonication in ultrapure water (Milli-$Q$, resistivity 18.2 $\mathrm{M}\cdot\Omega\cdot\mathrm{cm}^{-1}$), leading, after centrifugation, to 50 $\mu$L of a Janus colloidal solution at $\sim$0.05%v/v (about $10^9$ particles/mL). Such Janus particles were shown to self-propel in a $H_2O_2$ solution, due to the dismutation of this chemical on the platinum covering half of the colloids [14]. The properties of this colloidal suspension are then investigated in a dedicated microfluidic device, sketched in Figs. 1(b) and 1(c). It is made of a circular microfluidic chamber (diameter

 

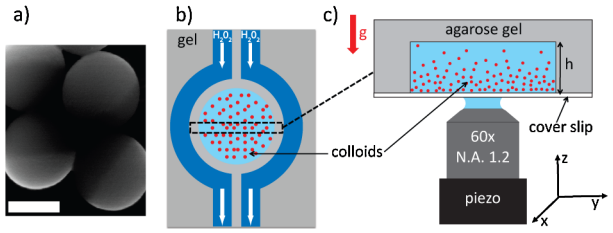


FIG. 1 (color online). (a) SEM picture of Janus, platinum-latex, colloids (scale bar 500 nm). (b) Sketch of the experimental setup: a circular microfluidic chamber (diameter $\Phi = 650\ \mu$m, height $h \sim 80\ \mu$m) molded in agarose gel (gray areas) contains the 1 $\mu$m Janus colloids. $H_2O_2$ feeding is achieved by constant circulation (40 $\mu$L/ min flow rate) in side channels (dark blue). (c) The active colloidal suspension is observed through a piezo-driven high numerical aperture objective (Nikon, Water immersion 60 ×, NA = 1.2) mounted on an inverted microscope.

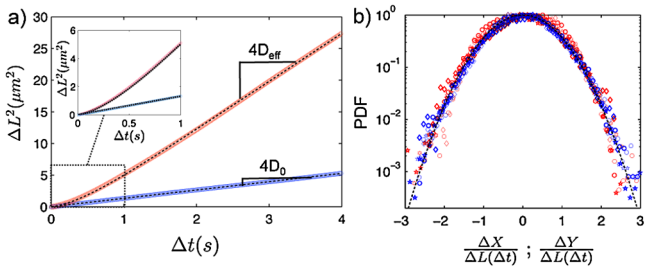


FIG. 2 (color online). (a) Experimental mean squared displacements $\Delta L^2(\Delta t)$ for bare (blue) and active colloids (red) in 7.5% $H_2O_2$ solution. *Inset:* zoom on the short-time regime. Bare colloids (bottom) show standard diffusion ($\Delta L^2$ linear in time), while the mean squared displacement of active colloids is fitted according to Eq. (1). The measured diffusion coefficients are $D_0 = 0.34\ \mu$m$^2$/s for bare and $D_{\text{eff}} = 1.9\ \mu$m$^2$/s for active colloids. (b) PDF of particle displacements along $x$ and $y$, $\Delta X = X(\Delta t) - X(0)$ (same for $Y$) for various lag time $\Delta t$ as a function of the normalized displacements, $\Delta X/\Delta L(\Delta t)$ (same for $Y$). $\Delta t = 0.3s$ (★), $1s$ (○), $3s$ (◇) for bare (blue) and active colloids (red) in a solution of 7.5% of $H_2O_2$. The dashed lines is the Gaussian curve.

$\Phi = 650\ \mu$m, height $\simeq 80\ \mu$m, volume $V \simeq 30$ nL) molded in agarose gel [19,21], and surrounded by two side channels separated by 125 $\mu$m gel walls. The central chamber is initially filled with Janus colloids, while $H_2O_2$ solution at concentration $C_0$ is continuously circulated in lateral channels. This gel microsystem ensures a constant renewal of $H_2O_2$ fuel and removal of chemical waste products ($O_2$) by diffusion through hydrogel walls from the infinite reservoir and sink constitued by the circulating lateral channel. Homogeneity of the measurements over the chamber was checked. Altogether this provides a convection-free environment in the colloids chamber with stable chemical conditions over hours, allowing to study solutions of active colloids (while a similar study would be precluded in a capillary due to production of oxygen bubbles).

*Colloid microdynamics.*—First, the dynamics of individual active colloids is investigated using high speed tracking measurements to resolve temporally the different dynamical regimes (see below). For various $H_2O_2$ concentrations $C_0$, the two-dimensional ($x$, $y$) motion of colloids is recorded with a high speed camera (Phantom V5) at 100 Hz and trajectories are extracted with a single particle tracking algorithm (Spot Tracker, Image $J$) [22]. The mean square displacement of the colloids is obtained as $\Delta L^2(\Delta t) = \langle(\vec{R}(t + \Delta t) - \vec{R}(t))^2\rangle$ where $\vec{R}(t)$ is the (2D) instantaneous colloid position and the average is performed over time for each individual trajectory and then over an ensemble of trajectories (typically 20). In Fig. 2 we plot $\Delta L^2$ as a function of lagtime for bare (nonactive) and active colloids in a $H_2O_2$ solution, confirming the impact of injected chemical power on the individual motion of the colloids, in agreement with Ref. [14]. For the bare (nonactive) colloids, the dynamics is purely diffusive with a diffusion coefficient $\Delta L^2/4\Delta t = D_0 = 0.34 \pm 0.02\ \mu$m$^2$/s, which is found to be reproducible and independent of the $H_2O_2$ concentration and slightly lower than the Stokes-Einstein estimate. The same value and behavior is obtained for Janus colloids in the absence of the $H_2O_2$ fuel. For the Janus active colloids in a $H_2O_2$ solution, the mean square displacement differs drastically from the equilibrium diffusive dynamics and strongly depends on the fuel concentration. The colloid exhibits ballistic motion at short times, $\Delta L^2(\Delta t) \sim V^2\Delta t^2$, while at longer times a diffusive regime, $\Delta L^2(\Delta t) \sim 4D_{\text{eff}}\Delta t$, is recovered with an effective diffusion coefficient $D_{\text{eff}}$ much larger than the equilibrium coefficient $D_0$. As discussed in [7,14], the active colloids are expected to perform a persistent random walk, due to a competition between ballistic motion under the locomotive power (with a constant swimming velocity $V$), and angular randomization due to thermal rotational Brownian motion. The transition between the two regimes occurs at the rotational diffusion time $\tau_r$ of the colloids, $\tau_r = 8\pi\eta R^3/k_BT$ ($R$ colloid radius). The characteristic ballistic length scale is accordingly $a = V \times \tau_r$. For time scales long compared to $\tau_r$, the active colloids therefore perform a random walk with an effective diffusion $D_{\text{eff}} = D_0 + V^2\tau_r/6$. The full expression of the mean squared displacement at any time is obtained as [14]

$$\Delta L^2(\Delta t) = 4D_0\Delta t + \frac{V^2\tau_r^2}{3}\left[\frac{2\Delta t}{\tau_r} + e^{-2\Delta t/\tau_r} - 1\right] \quad (1)$$

(where a prefactor in [14] has been corrected). We fit the experimental $\Delta L^2(\Delta t)$ using Eq. (1) with the propulsion velocity $V$ as a free parameter, while the value of $D_0$ is taken from the equilibrium diffusion coefficient measured in water, and with a single the value $\tau_r = 0.9$ s, in reasonable agreement with its Stokes expectation. As shown in Fig. 2(a), an excellent agreement with the experimental results is found. More sophisticated descriptions of the individual dynamics have been proposed, taking, e.g.,

into account fluctuations of the particle speed $V$ [23], or long-time correlations due to chemical relaxation [24]. However, in the explored regimes, the above simplified descriptions is found to account consistently for our experimental results. Under the present conditions, the measured propulsion velocities $V$ range from 0.3 $\mu$m/s to 3.3 $\mu$m/s. In the following we use this measure of $D_{\rm eff}$ as a probe of the colloidal 'activity'. Finally, we have also measured the probability distribution function (PDF) of the colloid displacement along both $x$ and $y$ directions, see Fig. 2(b), both for bare (blue) and active (red) colloid particles. In both cases, the PDF fits very well to a Gaussian with variance $\Delta L^2(\Delta t)$ given in Eq. (1). Although departures from a Gaussian are expected at short time for the persistent random walk, these are within experimental uncertainty.

*Sedimentation of active particles.*—We now turn to the investigation of an assembly of such active colloids, probed in a sedimentation experiment, in the same spirit as the historical Jean-Perrin experiment [20]. At thermal equilibrium with a bath at temperature $T$, a dilute population of colloids with (buoyant) mass $m$ under gravity $g$ exhibits a steady Boltzmann distribution profile $\rho(z) = \rho_0 \exp(-z/\delta_0)$ with $\delta_0 = k_B T/mg$ the sedimentation length, which balances gravitational and thermal energy. Alternatively this density profile can be seen as the stationary solution of the Smoluchowski diffusion-convection equation, $\partial_t \rho + \nabla \cdot J = 0$, with $J = -D_0 \nabla \rho + \mu mg \rho$ the particle flux, and $D_0$, $\mu$ the colloids diffusion coefficient and mobility. This leads to the fluctuation-dissipation relationship $D_0 = k_B T \mu$. In order to explore the validity of these concepts for the out-of-equilibrium active suspension [17], we have measured—simultaneously to the individual particle tracking experiments—the density profiles $\rho(z)$ of the colloids in the microfluidic chamber, for various fuel concentration $C_0$. Colloids profiles are measured by scanning the chamber using a piezo-mounted microscope objective (PIFOC P-725.2CD, Physik Instrumente). At each altitude $z$, a stack of images with lateral dimensions 150 × 200 $\mu$m is acquired at 0.3 Hz with a fluorescence camera (Orca, Hamamatsu). On each stack, image analysis is performed with Matlab: first the maximum fluorescence intensity $I_{\rm foc}$ is determined from "in-focus" colloids, then a $0.3 I_{\rm foc}$ threshold criterion is applied in order to discard out-of-focus colloids, thus defining a slice with thickness of $\pm 2$ $\mu$m [25]. A stack of 100 images is used to obtain a good statistical convergence. Overall this allows to obtain the average number of colloids at each altitude $z$. Note that adsorption of the colloids on the bottom surface was found to bias the density profiles for small altitudes and we thus discarded data from the first four microns. The results of these "Jean-Perrin" experiments are presented in Fig. 3. We have checked that a *stationary* state of the sedimentation profile is reached. As shown in Fig. 3, the density profiles of the active colloidal suspension $\rho(z)$ is decreasing with the altitude $z$ and, as in the thermal case, can be very well fitted by an exponential decay $\rho(z) = \rho_0 \exp(-z/\delta_{\rm eff})$, where $\rho_0$ was used to normalize the different measurements. The sedimentation length $\delta_{\rm eff}$ is found however to depend strongly on the activity of the colloids: $\delta_{\rm eff}$ increases with an increased propulsion of the colloids, *i.e.* injected energy, as measured (independently) by their effective diffusion coefficient $D_{\rm eff}$. The exponential decay suggests that in the present limit of a dilute active suspension, the active colloids still obey an effective Smoluchowski equation, with the current replaced by $J = -D_{\rm eff} \nabla \rho + \mu mg \rho$. This predicts a sedimentation length in the form

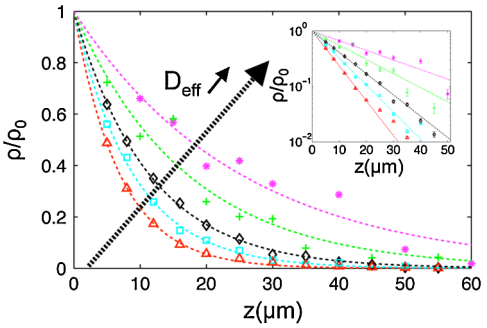


FIG. 3 (color online). Normalized density profiles $\rho/\rho_0(z)$ for the active colloidal suspension in stationary state, for increasing swimming activity, i.e., increasing $D_{\rm eff}$. Experimental data (symbols) are well fitted by an exponential decay $\rho(z) = \rho_0 \exp(-z/\delta_{\rm eff})$, with a sedimentation length $\delta_{\rm eff}$, which strongly depends on (and increases with) the swimming activity. Here $\delta_{\rm eff}$ varies from 6 $\mu$m at equilibrium up to 21 $\mu$m. *Inset:* Same data in a log-linear plot.

$$\delta_{\rm eff} = \frac{1}{v_T} D_{\rm eff}, \tag{2}$$

where $v_T = \mu mg$ is the sedimentation velocity.

We have checked this relationship by plotting the sedimentation length measured from the colloid density profiles, against the effective diffusion coefficient measured in the individual tracking measurements. As shown in Fig. 4, the predicted proportionality between sedimentation length and effective diffusion coefficient is demonstrated experimentally for all propelling activities, with a proportionality constant which is furthermore found to agree with its expected value in Eq. (2). This effectively connects the micro-dynamics of the active colloids to their global stationary profile. Equation (2) can also be interpreted as a fluctuation-dissipation measurement of the effective temperature of the system [17], here defined as $k_B T_{\rm eff} = D_{\rm eff}/\mu = \delta_{\rm eff} mg$. As plotted in the inset of Fig. 4, effective temperatures for this active system are found to range between the ambient temperature up to $10^3$ K. This result is compared with the theoretical expectation for $T_{\rm eff}$,

$$k_B T_{\rm eff} = k_B T \left(1 + \frac{2}{9} {\rm Pe}^2\right) \tag{3}$$

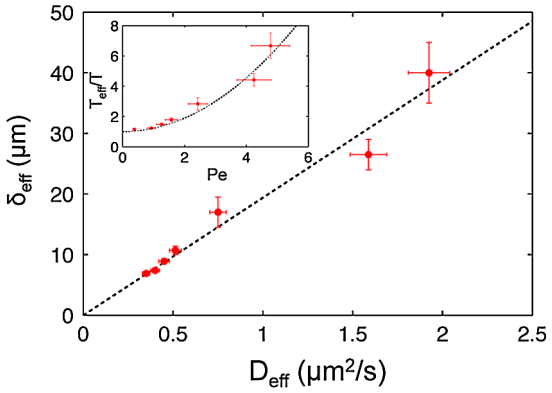


FIG. 4 (color online). Sedimentation length $\delta_{\mathrm{eff}}$ as a function of effective diffusion $D_{\mathrm{eff}}$ extracted from Figs. 2 and 3. The dashed line is a linear fit, $\delta_{\mathrm{eff}} = \alpha \times D_{\mathrm{eff}}$ as expected from Eq. (2). The measured slope $\alpha = 19.5 \pm 2\ \mu\mathrm{m}^{-1} \cdot \mathrm{s}$ is furthermore in good agreement with the expected value $\alpha = 1/v_T = \delta_0/D_0 = 16.2 \pm 2.5\ \mu\mathrm{m}^{-1} \cdot \mathrm{s}$, with $\delta_0$ and $D_0$ measured independently in the absence of injected $H_2O_2$. Inset: Plot of the effective temperature (normalized to the ambient temperature), $T_{\mathrm{eff}}/T$, versus the motility Peclet number, $\mathrm{Pe} = V.R/D_0$. The dashed line is the theoretical expectation, Eq. (3).

obtained from Eqs. (1) and (2), together with the relationship $\tau_r = 4R^2/3D_0$. Here, the Peclet number is defined as $\mathrm{Pe} = VR/D_0$, and thus characterizes the particle activity. A good agreement with the experimental results is found, as shown in Fig. 4. The Peclet number is the physical relevant parameter for this active system and in line with recent predictions [7], it would be desirable to increase its value, hence the effective temperature of the active system, in order to exalt collective effects. Since Pe is expected to scale as $\mathrm{Pe} \sim R^2$, this can be done by increasing the size of the Janus colloid.

Our results show that in the present regime, the active colloids behave as "hot" colloids, with an effective temperature much larger than the bare temperature. In the "*run and tumble*" model of particles under external fields [8], this behavior is indeed expected in the regime where the swim speed $V$ is larger than the sedimentation velocity $v_T$, and we thus validate the theoretical expectations in this regime.

To conclude, we have proposed efficient experimental tools allowing to explore the properties of *active colloidal suspensions* under controlled and tunable conditions. This involves artificial chemically active colloids, studied in a dedicated gel microfluidic system. This allows to measure the effective temperature of the active particles on the basis of fluctuation-dissipation relationship. It is found to increase strongly with colloidal activity. This opens up many perspectives towards a thorough exploration of the out-of-equilibrium behavior of active supensions [1–8], which still requires an exhaustive experimental confrontation. But beyond, it is interesting to note that the present colloids not only interact via hydrodynamic flows, but also via *chemical* (chemotacticlike) interactions, through the dipolar spatial extension of the consumed fuel leading to diffusiophoretic interactions. This is expected to affect the many-body behavior of the suspension, with couplings which have not been considered up to now in the literature. Finally, it would be interesting to test the fluctuation-dissipation concepts to living microorganisms, such as bacteria colonies.

[1] R. A. Simha and S. Ramaswamy, Phys. Rev. Lett. **89**, 058101 (2002).
[2] T. Vicsek, A. Czirók, E. Ben-Jacob, I. Cohen, and O. Shochet, Phys. Rev. Lett. **75**, 1226 (1995).
[3] K. Kruse, J. F. Joanny, F. Jülicher, J. Prost, and K. Sekimoto, Eur. Phys. J. E **16**, 5 (2005).
[4] I. Llopis and I. Pagonabarraga, Europhys. Lett. **75**, 999 (2006).
[5] H. Chaté, F. Ginelli, and R. Montagne, Phys. Rev. Lett. **96**, 180602 (2006).
[6] L. Angelani, R. Di Leonardo, and G. Ruocco, Phys. Rev. Lett. **102**, 048104 (2009).
[7] A. Baskaran and M. C. Marchetti, Proc. Natl. Acad. Sci. U.S.A. **106**, 15 567 (2009).
[8] R. W. Nash, R. Adhikari, J. Tailleur, and M. E. Cates, Phys. Rev. Lett. **104**, 258101 (2010).
[9] J. Deseigne, O. Dauchot, and H. Chate, Phys. Rev. Lett., arXiv:1004.1499 [Phys. Rev. Lett. (to be published)].
[10] A. Kudrolli, Phys. Rev. Lett. **104**, 088001 (2010).
[11] K. C. Leptos, J. S. Guasto, J. P. Gollub, A. I. Pesci, and R. E. Goldstein, Phys. Rev. Lett. **103**, 198103 (2009).
[12] X.-L. Wu and A. Libchaber, Phys. Rev. Lett. **84**, 3017 (2000).
[13] S. Rafaï, L. Jibuti, and P. Peyla, Phys. Rev. Lett. **104**, 098102 (2010)
[14] J. R. Howse *et al.*, Phys. Rev. Lett. **99**, 048102 (2007).
[15] R. Dreyfus *et al.*, Nature (London) **437**, 862 (2005).
[16] W. F. Paxton *et al.*, J. Am. Chem. Soc. **126**, 13 424 (2004).
[17] D. Loi, S. Mossa, and L. F. Cugliandolo, Phys. Rev. E **77**, 051111 (2008).
[18] R. Golestanian, T. B. Liverpool, and A. Ajdari, Phys. Rev. Lett. **94**, 220801 (2005).
[19] J. Palacci, B. Abécassis, C. Cottin-Bizonne, C. Ybert, and L. Bocquet, Phys. Rev. Lett. **104**, 138302 (2010).
[20] J. Perrin, Ann. Chim. Phys. **8**, 1 (1909).
[21] S. Y. Cheng *et al.*, Lab Chip **7**, 763 (2007).
[22] F. Hediger *et al.*, IEEE Trans. Image Process. **14**, 1372 (2005).
[23] F. Peruani and L. G. Morelli, Phys. Rev. Lett. **99**, 010602 (2007).
[24] R. Golestanian, Phys. Rev. Lett. **102**, 188305 (2009).
[25] M. Born and E. Wolf, *Principle Of Optics* (Cambridge University Press, Cambridge, England, 1999), 7th ed.